

EB-GLS: An Improved Guided Local Search Based on the Big Valley Structure

Jialong Shi · Qingfu Zhang ·
Edward Tsang

Received: date / Accepted: date

Abstract Local search is a basic building block in memetic algorithms. Guided Local Search (GLS) can improve the efficiency of local search. By changing the guide function, GLS guides a local search to escape from locally optimal solutions and find better solutions. The key component of GLS is its penalizing mechanism which determines which feature is selected to penalize when the search is trapped in a locally optimal solution. The original GLS penalizing mechanism only makes use of the cost and the current penalty value of each feature. It is well known that many combinatorial optimization problems have a big valley structure, i.e., the better a solution is, the more the chance it is closer to a globally optimal solution. This paper proposes to use big valley structure assumption to improve the GLS penalizing mechanism. An improved GLS algorithm called Elite Biased GLS (EB-GLS) is proposed. EB-GLS records and maintains an elite solution as an estimate of the globally optimal solutions, and reduces the chance of penalizing the features in this solution. We have systematically tested the proposed algorithm on the symmetric traveling salesman problem. Experimental results show that EB-GLS is significantly better than GLS.

Keywords Combinatorial Optimization · Metaheuristics · Traveling Salesman Problem · Guided Local Search · Elitism

Jialong Shi
Department of Computer Science, City University of Hong Kong, Hong Kong
E-mail: jlshi2-c@my.cityu.edu.hk

Qingfu Zhang
Department of Computer Science, City University of Hong Kong, Hong Kong

Edward Tsang
Centre for Computational Finance and Economic Agents, School of Computer Science and Electronic Engineering, University of Essex, Colchester, UK

1 Introduction

Memetic algorithms [9] use Local Search (LS) to improve their efficiency. Usually the solutions LS stops at are locally optimal solutions. Guided Local Search (GLS) [31] is a strategy that can improve the efficiency of LS. By changing the guide function of LS, GLS guides a LS procedure escape from locally optimal solutions and find better solutions. In this paper, we propose and study some improvements of the basic GLS strategy. The improved search strategy can be used by the memetic algorithm in the future. Our improvements are based on the big valley structure assumption in combinatorial optimization problems.

To use GLS, one has to first define a set of features which a candidate solution may exhibit. When the LS procedure is trapped in a local optimum, some selected unfavorable features are penalized. The objective function is augmented by the accumulated penalties and then used to guide the further search to move out of the attraction region of this local optimum. How to select features to penalize is a major issue in GLS. The penalizing mechanism proposed in [31] only considers the cost and the current penalty value of each feature. Based on the “big valley” structure assumption in combinatorial optimization [5], this paper proposes to estimate how likely each feature appears in a globally optimal solution from the best solutions found so far, and then use such information to improve the penalizing mechanism of GLS. More specifically, our proposed GLS method, called Elite Biased Guided Local Search (EB-GLS), record a best solution found so far during the search. Features in this solution are assumed to have a high chance to be good, and their probabilities to be penalized are reduced by using a simple method. The symmetric Traveling Salesman Problem (TSP) is used as a test suite to study the proposed EB-GLS in this paper. Our aim is not to develop the best algorithm for the TSP, but to illustrate that our modification can significantly improve the performance of GLS.

This paper is structured as follows. Section 2 presents the GLS procedure for the TSP. Section 3 introduces the recent works on designing an improved version of GLS. Section 4 discusses the big valley structure in the symmetric TSP. Section 5 presents the EB-GLS procedure for the symmetric TSP. To investigate whether or not EB-GLS achieves its design goal, Sections 6 and 7 compares EB-GLS and GLS experimentally. Our experiments are conducted on symmetric TSP instances from the TSPLIB and randomly generated symmetric TSP instances. Section 8 concludes the paper.

2 Guided Local Search

2.1 Traveling Salesman Problem

Let $G = (V, E)$ be a fully connected graph where V is its node set and E the edge set, and let $c_e > 0$ be the cost of $e \in E$. A tour s in G is a cycle passing

through every node in V exactly once and its cost is defined as:

$$g(s) = \sum_{e \in s} c_e. \quad (1)$$

A node in G can be interpreted as a city and c_e as the travel cost from the source node of edge e to its destination node. $g(\cdot)$ is the objective function. The goal of the Traveling Salesman Problem (TSP) is to find a tour with the smallest g value. The TSP is one of the most widely used NP-hard test problems in the area of heuristics. There are many different TSP variants. This paper considers the symmetric TSP, where G is undirected, i.e., the cost of travel from node A to node B is the same as that from B to A . We choose test instances from the best known TSPLIB [26] in our experimental studies. The instances in TSPLIB have known globally optimal costs. The dimensionality of a instance in TSPLIB is reflected by its name. For example, the dimensionality of the instances att532 is 532. We denote the set of all the tours in G as S , which is the solution space of the TSP.

2.2 Local Search

LS is a basic search and optimization technique. It can be used as an improved technology for many existing algorithms [11,17]. For example, LS has been successfully incorporated in the memetic algorithm to exploit the problem knowledge. LS defines a neighborhood for every candidate solution in the search space. It maintains one candidate solution and iteratively improves it. It searches the neighborhood of the current solution and moves to a neighboring solution which has a better guide function value. Most LS algorithms use the objective function of the problem in question as their guide function. LS stops and outputs the current solution as its final solution to the problem when all the neighbors are not better than the current solution according to the guide function. Since the neighborhood size is limited, LS usually stops at solutions that are not worse than their neighbors but not necessarily all other solutions in the search space, i.e. the locally optimal solutions.

Commonly-used LS heuristics for the TSP include 2-Opt heuristic, 3-Opt heuristic and Lin-Kernighan (LK) heuristic. All these algorithms are based on edge exchange. 2-Opt heuristic replaces two edges of the current solution by two other edges to obtain a neighboring solution. In 3-Opt heuristic, the number of edges to change is 3. In LK heuristic, the number of edges to change is variable.

2.3 Procedure of Guided Local Search

GLS is a simple penalty-based approach for helping a LS procedure to escape from local optima by dynamically adjusting its guide function. To use GLS, one needs to define a set of (solution) features for the given problem. For

example, in the TSP, the features can be defined as the edges between nodes. Given a candidate solution s and a feature i , function $I_i(s)$ is an indicator function of whether solution s exhibits feature i :

$$I_i(s) = \begin{cases} 1 & \text{if feature } i \text{ is in } s, \\ 0 & \text{otherwise.} \end{cases} \quad (2)$$

In GLS, each feature has a cost and a penalty. The cost is related to the objective function g . For example, in the TSP the cost of a feature is the cost of the corresponding edge. The penalties of all features are initialized to be zero at the beginning. Unlike other LS heuristics, GLS does not use the original objective function $g(\cdot)$, but function $h(\cdot)$ as its guide function for its LS procedure. Function $h(\cdot)$ is defined as:

$$h(s) = g(s) + \lambda \sum p_i I_i(s), \quad (3)$$

where λ is the parameter that controls the penalizing strength, p_i is the current penalty value of feature i . We call $h(\cdot)$ the augmented objective function.

GLS starts from an initial solution and executes a LS at each iteration using $h(\cdot)$ as its guide function. Once the LS stops at a local optimum s_* . GLS adjusts $h(\cdot)$ by increasing the penalties of one or more selected features in s_* . To do so, GLS defines the utility of each feature i , $util_i$ as

$$util_i(s_*) = I_i(s_*) \cdot \frac{c_i}{1 + p_i}, \quad (4)$$

where c_i is the cost of feature i . GLS selects the features with the highest utility value, and increases their penalties by 1. Then a new iteration starts from s_* . The pseudocode of GLS is shown in Algorithm 1. Inputs are the objective function g , the GLS parameter λ , the feature set M and the cost of each feature $i \in M$.

GLS conducts LS based on the augmented objective function $h(\cdot)$, which is different from the original objective function $g(\cdot)$. Hence GLS has to record the best solution found so far with regard to g . After each move of LS, GLS will check whether the g value of the new solution is lower than that of the recorded best solution, if so, the recorded best solution will be updated.

GLS has been successfully applied to the TSP [30]. To apply GLS to the TSP, we set edges as features and the costs of edges as the costs of features. Therefore, $M = E$. In this paper, we use 2-Opt as the LS heuristic of GLS on the TSP, because according to [30] GLS performs better with 2-Opt, especially when it is combined with the Fast Local Search (FLS) strategy [4,30]. In addition, using the 2-Opt LS heuristic makes our proposed algorithm easy to be implemented by other researchers.

2.4 Remarks

At each iteration, GLS performs a LS procedure and tries to escape from the encountered local optimum, which is similar to a well-known metaheuristic,

Algorithm 1 Guided Local Search

```

1: input:  $g, \lambda, M, c$ 
2:  $j \leftarrow 0$ 
3:  $s_0 \leftarrow$  random or heuristically generated solution.
4: for  $i = 1 \rightarrow |M|$  do
5:    $p_i \leftarrow 0$ 
6: end for
7: while !StoppingCriterion do
8:    $h \leftarrow g + \lambda \sum p_i I_i$ 
9:    $s_{j+1} \leftarrow$  LocalSearch( $s_j, h$ )
10:  for  $i = 1 \rightarrow |M|$  do
11:     $util_i \leftarrow I_i(s_{j+1}) \cdot c_i / (1 + p_i)$ 
12:  end for
13:  for each  $i$  such that  $util_i$  is maximum do
14:     $p_i \leftarrow p_i + 1$ 
15:  end for
16:   $j \leftarrow j + 1$ 
17: end while
18:  $s_* \leftarrow$  the best solution found with respect to  $g$ 
19: return  $s_*$ 

```

Iterated Local Search (ILS) [16]. ILS tries to escape from the current local optimum by perturbation, as illustrated in Fig. 1(a). GLS tries to escape from the current local optimum by increasing penalty on it. The increased penalty changes the guide function of GLS, which can be seen as “lifting” the local optimum, as illustrate in Fig. 1(b). The comparison results in [30] show that GLS performs better than ILS under the same computation cost. This means that in GLS the changed guide function improves the efficiency of the LS procedure. This is due to the well-designed penalizing mechanism of GLS. In (4), a feature with low cost c and the high current penalty value p are regarded as good. Good features in the current solutions will have little chance to be penalized. Here we analyse the design of (4) based on the knowledge (information) it learns during the search. The basic consideration in (4) is:

- **Use of a priori problem specific knowledge:** The goal of the TSP is to minimize the total cost of the tour. It is very natural to encourage to use low-cost features (i.e., edges in the TSP).
- **Use of online knowledge learned from the search:** If a feature exhibited in the current solution has a high penalty value, it implies that this feature has been penalized for many times. Such a feature is likely to be part of a good solution since it has exhibited in many locally optimal solutions of h .

The online knowledge used in GLS is the current penalty value of features. We believe that other forms of online knowledge can be exploited to improve estimation of goodness of a feature. This paper represents our effort along this line. Our work in this paper is based on the so called big valley structure hypothesis in combinatorial optimization.

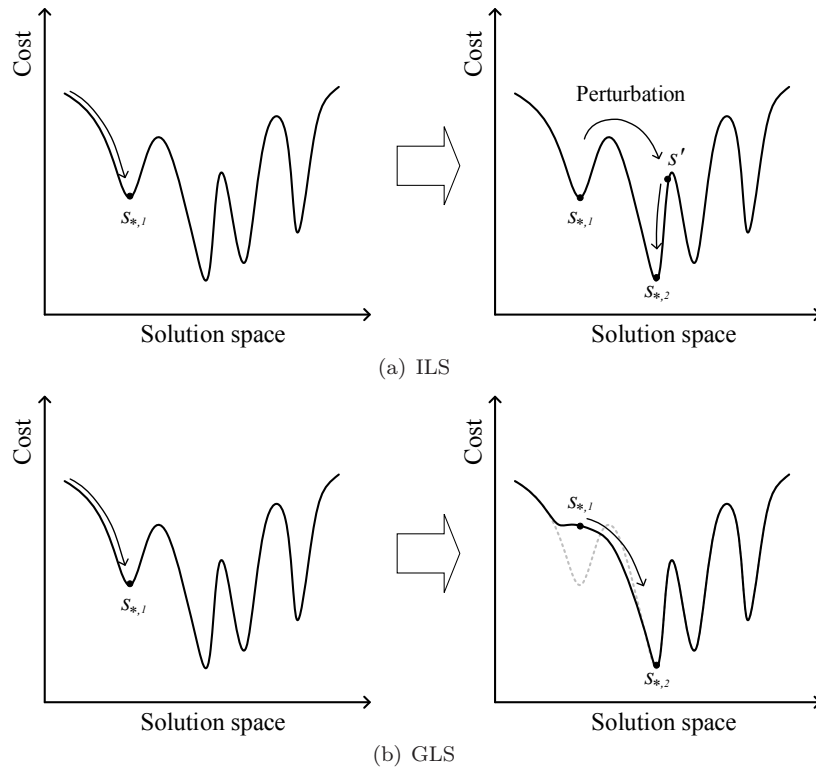


Fig. 1 The comparison between ILS's procedure and GLS's procedure

3 Literature Review

Besides the TSP, GLS has been successfully applied to many other optimization problems [31]. In addition, a number of variants and hybrid algorithms based on GLS have been proposed.

Guided Genetic Algorithm (GGA) [15] is a hybrid algorithm of GLS and Genetic Algorithm (GA). In GGA, when GA does not find an improved solution for a number of generations, the penalizing mechanism of GLS will be executed to change the guide function of GA. GGA is different from the Stepwise Adaptation of Weights (SAW) mechanism [7] which also changes the guide function of EA. When SAW increases penalties (weights) on the best individual, it increases penalties on all the violated constraints. When GGA increases penalties on the best individual, it only increases penalties on the features that have the largest $util$ value, and $util_i = c_i/(1 + p_i)$ is related to the historical penalty p_i . Hence, compared to SAW, the penalizing mechanism of GGA (which comes from GLS) considers the historical penalties to avoid penalizing a feature too many times. In the works of Mills et al. [22], two extended versions of GLS are proposed. The first one involves the aspiration criteria, which means ignoring the penalties if a move can

produce a new best solution. The second extended GLS allows random move from the neighbourhood when certain conditions are satisfied. Basharu et al. [3] proposed a modified GLS to solve the distributed constraint satisfaction problems, which is called Distributed GLS (Dis-GLS). In Dis-GLS, additional heuristics are introduced so that it can handle distributed scenarios. Tao and Haubrich [27] proposed a hybrid algorithm of GLS and Large Neighborhood Search (LNS) for the planning of medium-voltage power distribution systems, in which GLS and LNS are performed in different phases. In the GLS implementation proposed by Zhong and Cole [34], the features whose utilities are larger than a certain value are penalized and the penalties have an upper bound. In the work of Mester and Braysy [21], a hybrid algorithm of GLS and Evolution Strategies (ES) called Active Guided Evolution Strategies (AGES) is proposed. In AGES, when no improvement have been made for a user-defined number of iterations, the penalties are cleared and the search is restarted from the historical best solution. Guided Tabu Search (GTS) [28] is a hybrid algorithm of GLS, Variable Neighborhood Search (VNS) and Tabu Search (TS). In GTS, the guide function of TS is the objective function augmented by the penalty terms, which is same as that in GLS. In addition, GTS uses a new utility function $util_i = (c_i/avg_i)/(1 + p_i)$, in which the term avg_i can be considered the average cost of the other features related to feature i . The penalties on features are temporary and will be cleared after a certain tenure. In a variant of GTS [32], the costs of the features with the largest utility will be multiplied by 2, and restore to the original values after a given tenure. In the GLS implementation developed by Vansteenwegen et al. [29], when GLS is in a local optimum, it penalizes the included features with the highest “disutility” and rewards the non-included features with the highest utility. Here the principle of calculating utility and disutility is same as that of GLS.

GLS also has been applied to multi-objective optimization problems. In the related works, a multi-objective version of GLS called Guided Pareto Local Search (GPLS) [2] and a hybrid of GLS with MOEA/D [1] are proposed. However, in this paper we only discuss the possible improvement of GLS on single-objective optimization problems.

In the aforementioned variants and hybridizations of GLS, not much effort has been done to enhance the penalizing mechanism of GLS. In GTS, the penalizing mechanism considers the relative magnitude of feature cost through dividing the term avg_i . But there is no systemic experiment to prove that this modification in GTS can bring significant performance improvement. In [29], the features not included in current local optimum undergo an inverse version of the penalizing mechanism, but no systemic experiment study is done too. In this paper, we propose an enhanced penalizing mechanism of GLS by exploiting the big valley assumption. We also conduct systemic experiments to show that the modified penalizing mechanism can improve the performance of GLS on the symmetric TSP.

4 Big Valley Structure

Boese [5] presents a scatter plot of different local optima of the TSP instance att532 to illustrate its landscape. The following bond distance between two solutions s_1 and s_2 :

$$\text{distance}(s_1, s_2) = |\{e \in E | e \in s_1 \wedge e \notin s_2\}| \quad (5)$$

is used in his studies. He observed that there is a strong correlation between the distance of a solution to a global optimum and its cost. He call this phenomenon the big valley structure. Kauffman [14] observed the similar phenomenon in the NK landscapes with small K values, which is called ‘‘Massif Central’’. Jones and Forrest [12,13] also studied the relationship between the solution cost (which they call fitness) and the distance to the global optimum. They introduced fitness distance correlation (FDC) to measure the correlation between the solution quality and the distance to the nearest global optimum:

$$\text{FDC}(g, d_{opt}) = \frac{\text{cov}(g, d_{opt})}{\sigma(g)\sigma(d_{opt})}, \quad (6)$$

where g is the objective function value, i.e. the cost of solution, d_{opt} is the distance to the nearest global optimum, $\text{cov}(\cdot)$ denotes the covariance and $\sigma(\cdot)$ denotes the standard deviation. They suggested that FDC should be explored in algorithm design. Merz and Freisleben [19] conducted fitness landscape analysis on several TSP instances and found out that the fitness and the distance to the optimum are highly correlated for most instances. The big valley structure has also been reported in other combinatorial optimization problems, such as the maximum satisfiability [33], the unconstrained binary quadratic programming [20], the quadratic assignment problem [18], the flowshop scheduling [25], and others.

Although the big valley structure has been reported in many publications for a wide range of problems, however there is no uniform and strict definition for the big valley structure. In some publications, the big valley structure means that the global optima and local optima are clustered in a small region of the solution space. Some other publications mean high correlation between the cost and the distance to the nearest global optimum.

In this paper, we say that a TSP instance has a big valley structure when the following two requirements are met.

- If there are multiple globally optimum solutions, the mean bond distance between two global optima is significantly smaller than the mean distance between two randomly selected solutions, i.e. $N/2$. In other words, the global optima are located in a small region of the solution space, which can be seen as the ‘‘bottom’’ of the big valley, and
- There is a strong correlation between the cost of a solution and its distance to the nearest global optimum, i.e., the FDC value is relatively large.

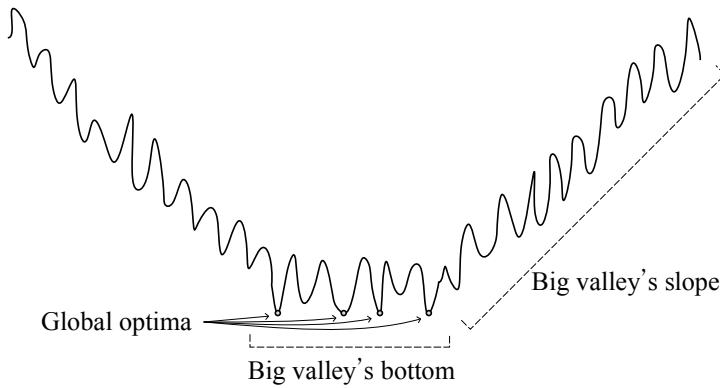


Fig. 2 Depiction of the big valley structure defined in this paper

Fig. 2 illustrates the big valley structure we mean in this paper.

Let's consider the TSP instance att532 with 532 nodes. According to [8, 23], It has two different global optima, and the bond distance between these two global optima is 2. Thus it meets the first requirement. To study if it meets the second requirement, we have executed 1,000 times of GLS and 1,000 times of EB-GLS (the GLS variant proposed in this paper) on att532 independently from randomly generated solutions. During each run, when the current best solution changes, the new best solution is recorded. In total, 292,714 solutions have been recorded. Fig. 3 is the scatter plot of these solutions. The FDC value of the solutions shown in Fig. 3 is 0.83. It is clear that it meets the second requirement. Therefore, the instance att532 has the big valley structure, which is consistent with the statement made by Boese [5].

However, the big valley structure does not hold in all the TSP instance. We have conducted the same experiments on nine other instances from the TSPLIB, and found that eight instances have the big valley structure while one instance does not. The experiment results on the eight instances can be found in the Appendix. Here we focus on the instance that does not have the big valley structure, u2319. On u2319, 2,000 runs of GLS/EB-GLS found total 2,000 different global optima, which means that u2319 have at least 2,000 global optima. The mean distance between these global optima is 884, in which the minimum distance is 777 and the maximum distance is 992. Hence the mean distance between the global optima is not significantly smaller than the mean distance between two randomly selected solutions in u2319, i.e. $2319/2 = 1160$. This means that the global optima are widely scattered in the solution space. Thus we claim that u2319 does not satisfy the first requirement of the big valley structure.

In the following, we propose an enhanced GLS algorithm which exploits the big valley structure assumption. We will show that the proposed algorithm performs significantly better than GLS on att532 (the instance that has the big valley structure). Meanwhile its performance does not drastically deteriorate on u2319 (the instance that does not have the big valley structure).

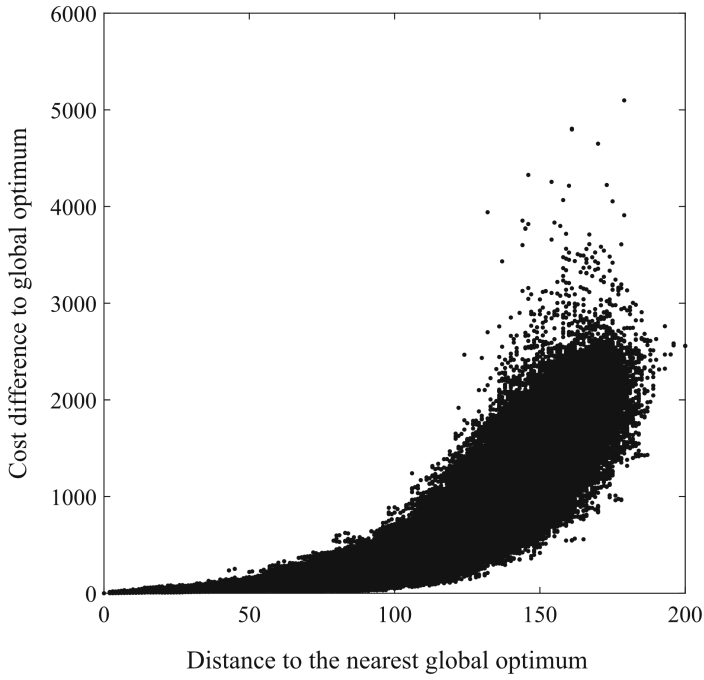


Fig. 3 The recorded solutions during 1,000 runs of GLS and 1,000 runs of EB-GLS on att532. The cost difference to the globally optimal cost (vertical axis) is plotted against the distance to the nearest globally optimal solution (horizontal axis). There is a clear correlation between the cost and the distance to the nearest global optimum.

5 Elite Biased Guided Local Search

5.1 Procedure

Our improved GLS algorithm called Elite Biased Guided Local Search (EB-GLS) maintains an elite solution s_e (i.e. a high-quality solution) as an estimate of the global optimum, and uses a different *util* formula. The new *util* formula is:

$$util_i(s_*) = \begin{cases} I_i(s_*) \cdot \frac{c_i}{1 + p_i}, & \text{if } s_e \text{ includes feature } i; \\ I_i(s_*) \cdot \frac{c_i}{1 + p_i} \cdot w, & \text{otherwise,} \end{cases} \quad (7)$$

where w is a predefined constant larger than 1. Since $w > 1$, the features in s_e will have relatively small *util* values, hence the penalties imposed on the features in s_e are reduced. EB-GLS directly use the best solution found so far as s_e , so that no additional effort is introduced. Algorithm 2 is the pseudocode of EB-GLS. Compared to GLS (Algorithm 1), EB-GLS has an extra input parameter: w .

Algorithm 2 Elite Biased Guided Local Search

```

input:  $g, \lambda, M, c, w$ 
 $j \leftarrow 0$ 
 $s_0 \leftarrow$  random or heuristically generated solution in  $S$ 
for  $i = 1 \rightarrow |M|$  do
   $p_i \leftarrow 0$ 
end for
while !StoppingCriterion do
   $h \leftarrow g + \lambda \sum p_i I_i$ 
   $s_{j+1} \leftarrow$  LocalSearch( $s_j, h$ )
   $s_e \leftarrow$  historical best solution with respect to  $g$ 
  for  $i = 1 \rightarrow |M|$  do
    if  $s_e$  includes feature  $i$  then
       $util_i \leftarrow I_i(s_{j+1}) \cdot \frac{c_i}{(1+p_i)}$ 
    else
       $util_i \leftarrow I_i(s_{j+1}) \cdot \frac{c_i}{(1+p_i)} \cdot w$  /*  $w > 1$  */
    end if
  end for
  for each  $i$  such that  $util_i$  is maximum do
     $p_i \leftarrow p_i + 1$ 
  end for
   $j \leftarrow j + 1$ 
end while
 $s_* \leftarrow$  historical best solution with respect to  $g$ 
return  $s_*$ 

```

The efficiency and effectiveness of a search algorithm depend on how search effort is allocated in the search space, and balancing between exploitation and exploration. The aim of EB-GLS is to allocate more search effort on the search regions near to s_e by reducing the penalties on s_e . According to the big valley structure hypothesis, those regions are more likely to contain high-quality solutions, even the global optima. Meanwhile EB-GLS keeps updating s_e by the newly found better solutions to explore more promising regions and prevent the search process from stalling.

5.2 Some Implementation Notes

5.2.1 The update of s_e

At the early search stage, a best solution found so far may be not of high quality and thus can be far away from the global optima. On the other hand, too frequent update of s_e in EB-GLS is not necessary and may involve extra computation load. Based on these considerations, in our experimental studies, suppose the total runtime is T , we first run GLS for $10/T$ and then change to EB-GLS. We update s_e once every 100 executions of the LS procedure.

5.2.2 The values of λ and w

Following [30], we set

$$\lambda = 0.3 \cdot \frac{g(\text{first local optimum})}{N}, \quad (8)$$

where $g(\text{first local optimum})$ is the cost of the first local minimum. As to w , our pilot experiments show that EB-GLS is not very sensitive to w . We set $w = 2$ in this paper.

6 Behavior of Elite Biased Guided Local Search

EB-GLS aims at reducing penalties on the features in the global optima by exploiting the big valley structure. To investigate whether EB-GLS achieves this design goal, we conduct an experiment which records the behaviors of EB-GLS and GLS during the search. We select two instances, att532 and u2319, as the test instances. According to Section 4, att532 has a typical big valley structure, meanwhile u2319 does not have the big valley structure. In our experiment, we execute thousands of runs of GLS and EB-GLS on att532 and u2319. Each run ends only when the global optimal cost is achieved. The instance att532 only have two global optima, and the distance between those two global optima is 2, which means there are totally 534 different edges in the two global optima. Fig. 4 shows the 534 edges that belong to the two global optima of att532. The instance u2319 has more than 2,000 global optima and the mean distance among them is large, hence the edge number in the global optima set of u2319 is huge and hard to be visualized.

6.1 Experiment Settings

In our experiment, we execute 1,000 runs of GLS and 1,000 runs of EB-GLS. Each GLS run has a corresponding EB-GLS run which starts from the same initial solution. All the runs of GLS and EB-GLS stop only when a globally optimum is found. In both EB-GLS and GLS, the FLS strategy and the first-improvement LS strategy are applied. In EB-GLS implementation, the GLS is run for the first 10,000 iterations and then EB-GLS starts. s_e is updated once every 100 iterations. We have recorded the best solution found so far with regards to g after every 1,000 iterations in each run of these two algorithms.

6.2 Performance Metrics

On the instance att532, we measure the search performance of both GLS and EB-GLS by the following four metrics:

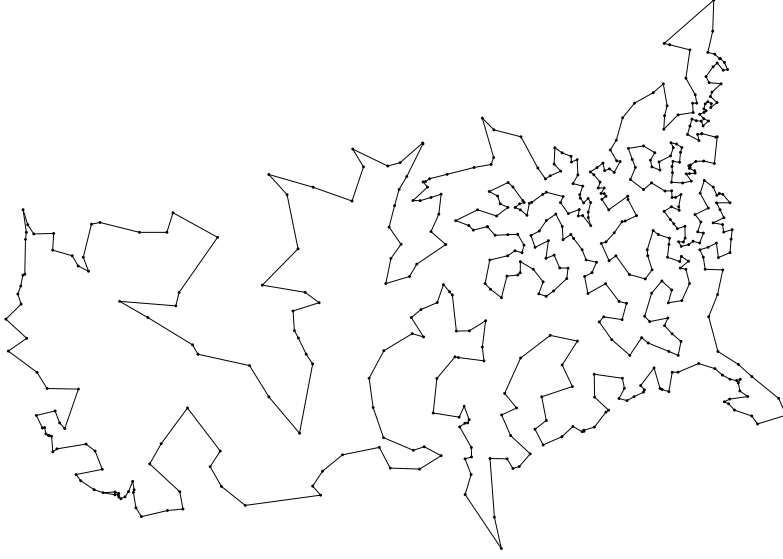


Fig. 4 Edges that belong to the two global optima of att532

- **Average Best Excess $\bar{\epsilon}$** : At the end of $1,000 \times j$ -th iteration in run k , the best excess $\epsilon_{j,k}$ is the excess of the best solution found so far:

$$\epsilon_{j,k} = \frac{\text{current best solution cost} - \text{globally optimal cost}}{\text{globally optimal cost}} \times 100\%. \quad (9)$$

The average best excess among all the 1,000 runs, $\bar{\epsilon}_j$, is defined as

$$\bar{\epsilon}_j = \frac{1}{1000} \sum_{k=1}^{1000} \epsilon_{j,k}. \quad (10)$$

When run k has found a global optimum with less than $1,000 \times j$ iterations, $\epsilon_{j,k}$ is set to be zero.

- **Average Distance to Global Optimum \bar{d}** : At the end of $1,000 \times j$ -th iteration in run k , $d_{j,k}$ is the distance (i.e., the number of different edges) between the best solution found so far and the final global optimum found in this run. The average distance \bar{d}_j over 1,000 runs is defined as:

$$\bar{d}_j = \frac{1}{1000} \sum_{k=1}^{1000} d_{j,k}. \quad (11)$$

Similar to the definition of $\bar{\epsilon}_j$, $d_{j,k}$ is set to be zero if run k has found a global optimum with less than $1,000 \times j$ iterations.

- **Average Ratio of Undesirable Penalties \bar{r}** : At each iteration in every run, each edge has a penalty value. In total, there are 534 different edges in the two global optima of att532. It is undesirable to penalize these edges. $r_{j,k}$ is defined as the ratio between the total penalty on those 534 edges over the total penalty on all the edges at the $1,000 \times j$ -th iteration in run k . In each algorithm, \bar{r}_j is the average of all the $r_{j,k}$ values in all the runs which have not found a global optimum at the end of $1,000 \times j$ -th iteration. \bar{r} reflects the probability of GLS/EB-GLS penalizing the 534 edges of the global optima. Obviously, everything being equal, a lower \bar{r} value reflects a more effective penalizing mechanism.
- **Average Ratio of Increased Undesirable Penalties \bar{r}_Δ** : From the $1,000 \times (j - 1)$ -th iteration to the $1,000 \times j$ -th iteration in run k , $r_{\Delta,j,k}$ is defined as the ratio between the increment of the total penalty on those 534 edges over the increment of the total penalty on all the edges during that 1,000 iterations. $\bar{r}_{\Delta,j}$ is the average of all the $r_{\Delta,j,k}$ values in all the runs which have not found a global optimum at the end of $1,000 \times j$ -th iteration. \bar{r}_Δ reflects the probability of GLS/EB-GLS penalizing the 534 edges of the global optima during every 1,000 iterations.

Since the number of global optima in u2319 is huge, and the number of the edges in the global optima is also huge, we only calculate the average best excess $\bar{\epsilon}$ in the experiment on u2319.

6.3 Experiment Results

6.3.1 Results on the instance with big valley structure: att532

Fig. 5 shows on att532 how the average best excess $\bar{\epsilon}$ of GLS and EB-GLS changes with the iteration. The 10,000th iteration, which is marked by a vertical solid line in Fig. 5, is the time when EB-GLS starts its own penalizing mechanism. Fig. 6 shows how the average distance to global optimum \bar{d} changes with the iteration in GLS and EB-GLS respectively.

From Fig. 5 and Fig. 6, it is clear that after EB-GLS starts using its penalty mechanism at the 10,000th iteration, EB-GLS performs much better than GLS in terms of both $\bar{\epsilon}$ and \bar{d} . It implies that the best solutions found by the EB-GLS runs have lower costs and are closer to the global optimum. EB-GLS can always keep its superiority.

Fig. 7 shows how the average ratio of undesirable penalties \bar{r} changes with the iteration in GLS and EB-GLS respectively. It shows the change over the first 50,000 iterations. All of the 1,000 GLS runs and 935 EB-GLS runs (the other runs have terminated within 50,000 iterations) are used to calculate \bar{r} in the first 50,000 iterations. It is obvious that \bar{r} decreases in both EB-GLS and GLS, which suggests that both algorithms are able to identify good features. However, Fig. 7(a) does not show any significant difference between EB-GLS and GLS in terms of \bar{r} . It is because \bar{r} is calculated based on the accumulated penalties. To see the difference more clearly, Fig. 7(b) plots the difference

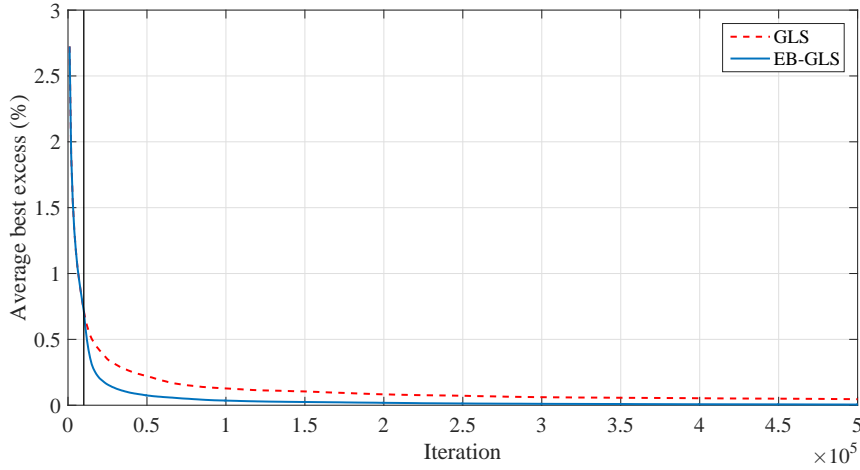


Fig. 5 The average best excess $\bar{\epsilon}$ of GLS and EB-GLS on the instance att532. $\bar{\epsilon}$ (vertical axis) is plotted against the iteration (horizontal axis)

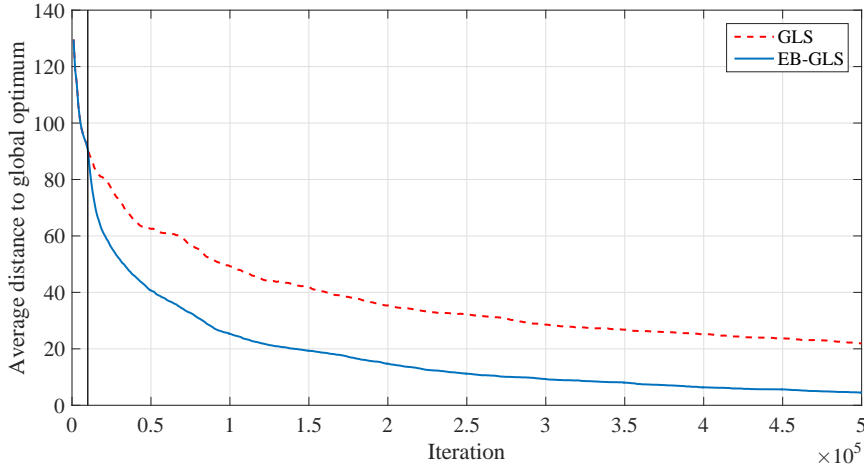


Fig. 6 The average distance to global optimum \bar{d} of GLS and EB-GLS on the instance att532. \bar{d} (vertical axis) is plotted against the iteration (horizontal axis)

between these two values. We can observe from it that after the 10,000th iteration, the \bar{r} value of EB-GLS is smaller than the \bar{r} value of GLS. This means that EB-GLS is less likely to penalize the edges of the global optima compared to GLS.

Fig. 8 shows how \bar{r}_Δ changes with the iteration in GLS and EB-GLS separately. From Fig. 8(a) and 8(b), it is evident that, after the 10,000th iteration, EB-GLS penalizes less global optima's edges than GLS. Especially at the 11,000th iteration, the \bar{r}_Δ value of EB-GLS is 38% smaller than that of

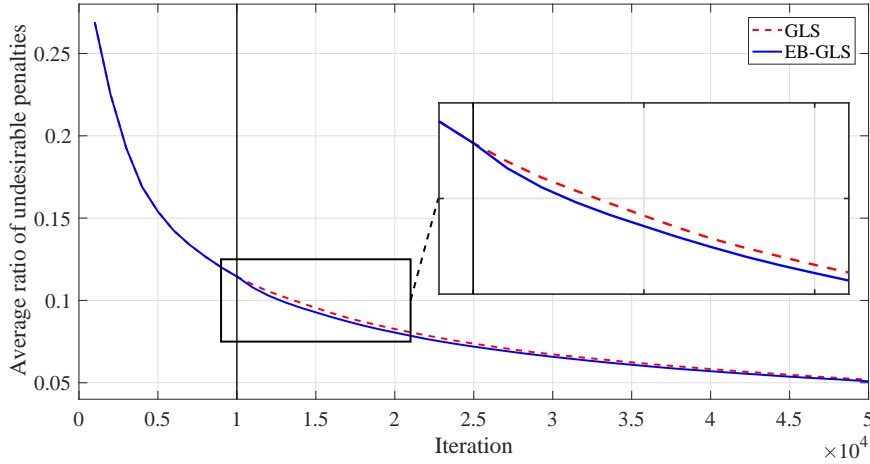
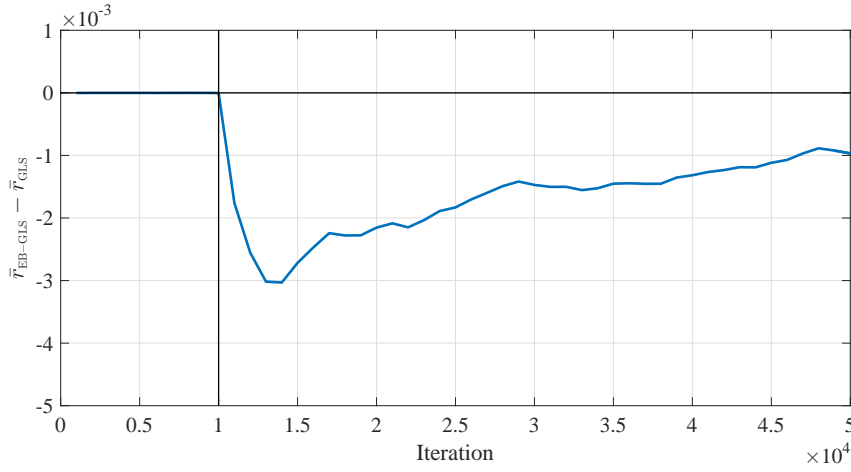
(a) $\bar{r}_{\text{EB-GLS}}$ and \bar{r}_{GLS} (b) $\bar{r}_{\text{EB-GLS}} - \bar{r}_{\text{GLS}}$

Fig. 7 The average ratio of undesirable penalties \bar{r} of GLS and EB-GLS on the instance att532. (a): \bar{r} is plotted against the iteration (horizontal axis). (b): $\bar{r}_{\text{EB-GLS}} - \bar{r}_{\text{GLS}}$ (vertical axis) is plotted against the iteration (horizontal axis)

GLS. However, after the 11,000th iteration, the \bar{r}_{Δ} value of EB-GLS increases until it reaches the same level of GLS's \bar{r}_{Δ} value. It is because, as the search progresses, the solutions found by EB-GLS is closer to the global optima than that of GLS (as shown in Fig. 6). This means the current solution of EB-GLS contains more common edges with the global optima than that of GLS. Since GLS/EB-GLS only penalizes the edges in its current solution, the chances of EB-GLS penalizing the edges in the global optima increases. It makes EB-GLS's \bar{r}_{Δ} increase. After the 15,000th iteration, the increase trend ends and

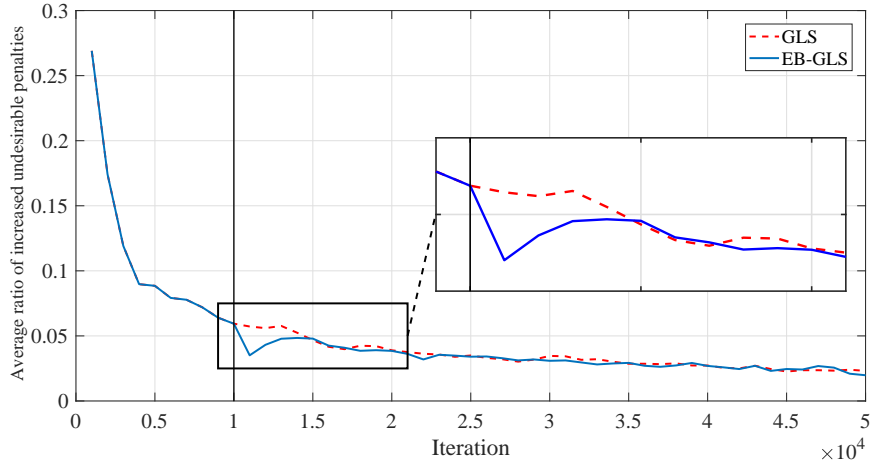
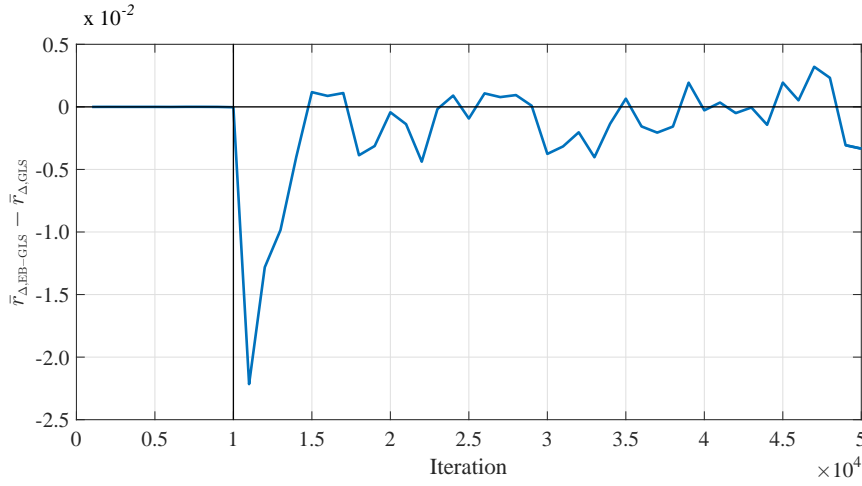
(a) $\bar{r}_{\Delta, \text{EB-GLS}}$ and $\bar{r}_{\Delta, \text{GLS}}$ (b) $\bar{r}_{\Delta, \text{EB-GLS}} - \bar{r}_{\Delta, \text{GLS}}$

Fig. 8 The average ratio of increased undesirable penalties \bar{r}_{Δ} of GLS and EB-GLS on the instance att532. (a): \bar{r}_{Δ} is plotted against the iteration (horizontal axis). (b): $\bar{r}_{\Delta, \text{EB-GLS}} - \bar{r}_{\Delta, \text{GLS}}$ (vertical axis) is plotted against the iteration (horizontal axis)

EB-GLS's \bar{r}_{Δ} is about the same as in GLS. However, considering that the current solution of EB-GLS contains more edges of the global optima than that of GLS, the similarity of the \bar{r}_{Δ} values of EB-GLS and GLS confirms the advantage of EB-GLS over GLS.

In summary, the design goal of EB-GLS, which is to exploit the big valley structure in order to reduce the probability of penalizing the edges of global optima, has been achieved. Although the probability of EB-GLS penalizing the edges in the global optima is only a little smaller than that of GLS (as

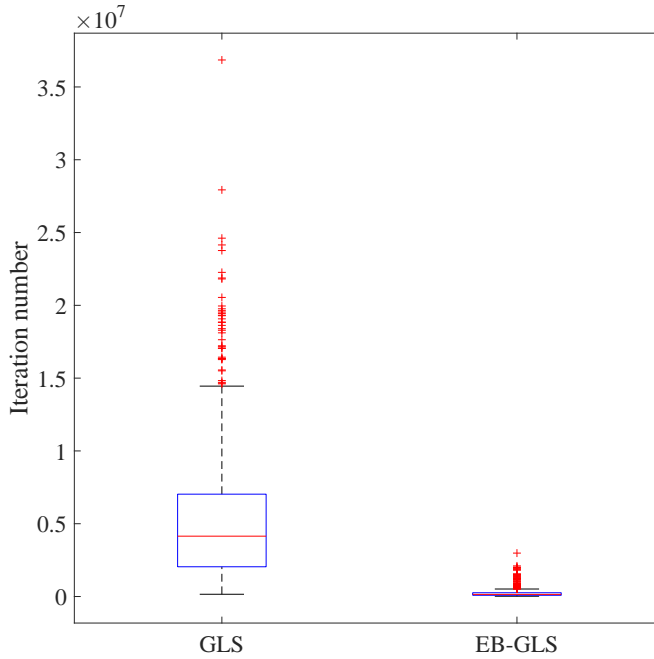


Fig. 9 The box plot of the iteration number GLS and EB-GLS take to find a global optimum on the instance att532

shown in Fig. 7(a)), this little difference endows EB-GLS with a significantly better performance. Fig. 9 is the box plot of the number of iterations GLS and EB-GLS take to find a global optimum on the instance att532. Based on the Mann-Whitnet U-test with a 0.05 significance level, we conclude that the total iteration number of EB-GLS is significantly smaller than that of GLS, which means that EB-GLS is significantly faster than GLS.

6.3.2 Results on the instance without big valley structure: u2319

Fig. 10 shows how the average best excess $\bar{\epsilon}$ changes with the iteration on u2319. We can see that, GLS's $\bar{\epsilon}$ value is lower than that of EB-GLS in the early phase of the search process. But as the search continues, the gap between the two curves become small. Fig. 11 is the box plot of the number of iterations GLS and EB-GLS take to find a global optimum on the instance u2319. In Fig. 11, the average iteration number GLS takes to find a global optimum is 1,643,358, while the average iteration number EB-GLS takes to find a global optimum is 1,481,367. We can see that, on the instance u2319 that does not have a big valley structure, the performance of EB-GLS does not drastically deteriorate.

Having say that, this experiment only proves that EB-GLS out-performs GLS on att532, and EB-GLS's performance does not drastically deteriorate

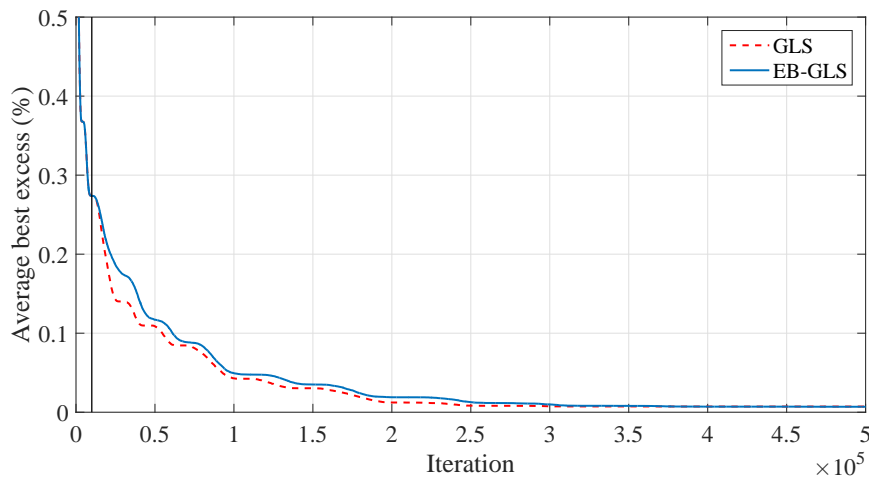


Fig. 10 The average best excess, $\bar{\epsilon}$, in GLS and EB-GLS. $\bar{\epsilon}$ (vertical axis) is plotted against the iteration (horizontal axis). Instance: u2319

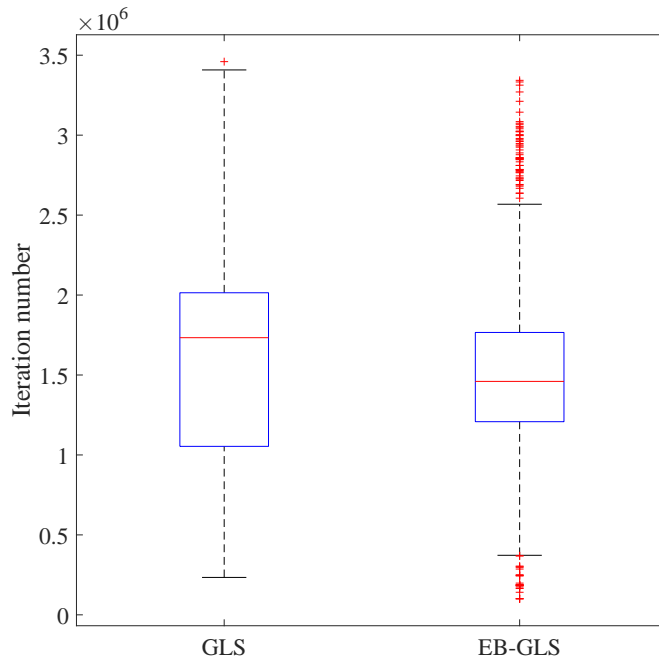


Fig. 11 The box plot of the iteration number GLS and EB-GLS take to find a global optimum on the instance u2319

on u2319. In the next section, we will compare the performances of EB-GLS and GLS on more instances, so as to fully assess the performance of EB-GLS against GLS.

7 Performance Comparison

In this paper, we argue that the original GLS can be improved by exploiting the big valley structure. To prove the effectiveness of our idea, in the following part, we compare the performance of EB-GLS and GLS on a large number of symmetric TSP instances. Our objective is not to obtain a best algorithm for the TSP, hence here we do not compare EB-GLS with the state-of-the-art TSP algorithms, such as LKH [10]. Comparative experiments are conducted on two kinds of instances: instances from TSPLIB and randomly generated instances. Both EB-GLS and GLS are implemented in GNU C++ with O2 optimizing compilation. The computing platform is two 6-core 2.00GHz Intel Xeon E5-2620 CPUs (24 Logical Processors) under CentOS 6.4.

7.1 Comparison on TSPLIB Instances

There are 111 symmetric TSP instances in TSPLIB. In this experiment we choose 109 instances as test instances. The instance linhp312 is excluded because it requests the solution to contain a fixed edge. The largest instance pla85900 is excluded because of the RAM limitation of our hardware.

7.1.1 Experiment settings

Most of the settings of this comparative experiment remain the same as the settings of the experiment introduced in Section 6, except the following:

- We execute GLS and EB-GLS 100 runs on each instance.
- Both algorithms stop when a global optimum is found or the predetermined maximum runtime is reached. For a TSP instance with N cities, the maximum runtime $T = \lceil N/10 \rceil$ seconds. For example, the maximum runtime on the instance fl1577 (which has 1577 cities) is 158 seconds.
- For the EB-GLS runs on the instances with not less than 1000 cities, we first run GLS for $\lfloor T/10 \rfloor$ seconds and then change to EB-GLS. For example, on the instance fl1577, the starting time of applying EB-GLS in the EB-GLS runs is the $\lfloor 158/10 \rfloor = 16$ th second. For the EB-GLS runs on the instances with less than 1000 cities, the EB-GLS mechanism starts at the beginning.

7.1.2 Experiment results

We use three metrics to measure the performance of GLS/EB-GLS. The first metric is the number of runs that successfully find a global optimum. The second one is the average best excess of all the 100 runs. The third one is the

Table 1 Comparison results between EB-GLS and GLS on the TSPLIB instances with not less than 1000 cities, the better metric values are marked by bold texts

Instance	Max Runtime (s)	Success of 100		Average Excess (%)		Excess P-value	Average Runtime (s)		Runtime P-value
		GLS	EB-GLS	GLS	EB-GLS		GLS	EB-GLS	
dsj1000	100	0	1	0.2821	0.0856 +	5.11e-34	100.00	99.99 ≈	3.22e-01
pr1002	101	0	82	0.0610	0.0009 +	1.43e-36	101.00	60.13 +	2.69e-29
si1032	104	0	20	0.0340	0.0139 +	1.04e-13	104.00	94.75 +	2.72e-06
u1060	106	0	48	0.0720	0.0080 +	2.05e-34	106.00	87.70 +	4.98e-15
vm1084	109	0	32	0.0638	0.0159 +	2.89e-31	109.00	87.72 +	9.14e-10
pcb1173	118	0	22	0.0737	0.0095 +	5.37e-34	118.00	103.85 +	7.58e-07
d1291	130	1	16	0.1196	0.0739 +	6.76e-07	128.86	119.78 +	1.80e-04
rl1304	131	0	76	0.0443	0.0261 +	2.19e-15	131.00	69.14 +	2.00e-26
rl1323	133	1	26	0.0748	0.0387 +	3.91e-09	132.82	116.38 +	2.16e-07
nrw1379	138	0	7	0.0896	0.0164 +	4.33e-34	138.00	134.60 +	7.31e-03
fl1400	140	0	1	0.5054	0.3119 +	1.44e-19	140.00	139.79 ≈	3.22e-01
u1432	144	53	93	0.0092	0.0020 +	9.41e-10	112.79	67.09 +	1.69e-12
fl1577	158	0	0	0.3325	0.2555 +	2.50e-07	158.00	158.00 ≈	-
d1655	166	0	5	1.0514	0.9681 +	2.46e-03	166.00	163.25 +	2.42e-02
vm1748	175	0	9	0.1350	0.0496 +	2.17e-31	175.00	171.31 +	2.23e-03
u1817	182	0	1	0.2220	0.1398 +	1.01e-16	182.00	181.93 ≈	3.22e-01
rl1889	189	0	3	0.2011	0.0753 +	1.24e-24	189.00	187.30 ≈	8.27e-02
d2103	211	0	0	0.1728	0.1339 +	6.09e-09	211.00	211.00 ≈	-
u2152	216	0	0	0.2776	0.1725 +	1.88e-15	216.00	216.00 ≈	-
u2319	232	30	6	0.0051	0.0068 -	1.06e-05	209.62	227.16 -	1.43e-05
pr2392	240	0	0	0.1429	0.0410 +	1.73e-26	240.00	240.00 ≈	-
pcb3038	304	0	0	0.2025	0.0732 +	8.08e-34	304.00	304.00 ≈	-
fl3795	380	0	0	2.1908	2.4098 ≈	8.87e-01	380.00	380.00 ≈	-
fm14461	447	0	0	0.2547	0.1175 +	2.79e-34	447.00	447.00 ≈	-
rl5915	592	0	0	0.5100	0.3941 +	1.92e-06	592.00	592.00 ≈	-
rl5934	594	0	0	0.7126	0.6214 +	3.53e-03	594.00	594.00 ≈	-
pla7397	740	0	0	0.4588	0.3834 +	1.27e-07	740.00	740.00 ≈	-
rl11849	1185	0	0	0.8366	0.7266 +	2.24e-06	1185.00	1185.00 ≈	-
usa13509	1351	0	0	0.8776	0.6231 +	7.17e-26	1351.00	1351.00 ≈	-
brd14051	1406	0	0	1.8110	1.6733 +	2.51e-06	1406.00	1406.00 ≈	-
d15112	1512	0	0	0.7742	0.5720 +	2.68e-27	1512.00	1512.00 ≈	-
d18512	1852	0	0	0.8098	0.7522 +	2.13e-09	1852.00	1852.00 ≈	-
pla33810	3381	0	0	1.2438	1.3276 -	3.18e-02	3381.00	3381.00 ≈	-

average real runtime of all the 100 runs. Table 1 shows the comparison results between EB-GLS and GLS on the 33 TSPLIB instances with not less than 1000 cities. The comparison results on the rest 76 TSPLIB instances can be found in the Appendix. In Table 1 the bold font means that one algorithm gets a better metric value than the other one. We perform Mann-Whitney U-test on the excess data and the runtime data respectively. In Table 1, the sign “+”(resp. “-”, “≈”) indicates that EB-GLS achieves better (resp. worse, equivalent) results than GLS using a Mann-Whitney U-test at the 0.05 significance level.

To compare the performances between GLS and EB-GLS, we use the “domination” concept from multi-objective optimization to judge which one is better. Through the statistical tests, if algorithm A is not significantly worse than algorithm B on all three metrics, and A is significantly better than B on at least one metric, then we state that A out-performs B. Among the 109 instances, EB-GLS out-performs GLS on 82 instances (75.23%), while GLS out-performs EB-GLS on only 6 instances (5.50%). Furthermore, among the 71 instances whose city numbers are not less than 150, EB-GLS out-performs GLS on 65 instances (91.55%), while GLS out-performs EB-GLS on only 2 instances (2.82%), u2319 and pla33810. In Section 4 we know that the instances u2319 does not have the big valley structure, which explains

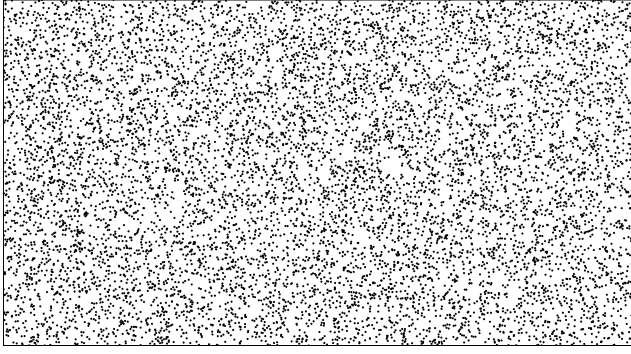


Fig. 12 City distribution in randc10000

why the performance of EB-GLS is worse than that of GLS on u2319. The other instance pla33810 contains a large number of nodes, hence it is difficult to investigate its landscape structure experimentally. In summary, from the above comparison results we can conclude that the overall performance of EB-GLS is better than the performance of GLS on most instances of TSPLIB.

7.2 Comparison on Randomly Generated Instances

In this experiment, GLS and EB-GLS is each executed on 10 randomly generated symmetric TSP instances.

7.2.1 Experiment settings

The 10 randomly generated instances all have 10,000 cities. These instances are named “randa10000”, “randb10000”, . . . , “randj10000”, respectively. For each instance, both the length and width of the map are randomly uniform number generated from the interval $(1 \times 10^5, 1.1 \times 10^6)$. the positions of 10,000 cities are uniformly distributed in the map. For example, Fig. 12 shows the city distribution in randc10000.

For each run on each test instance, the maximum runtime is 1,000 seconds, and in EB-GLS the starting time of applying EB-GLS is the 100th second. Since the global optima of these random instances are unknown, all runs stop only when the maximum runtime is reached. After that, the cost of the best solution found is recorded. The other experiment settings are same as that in the comparative experiment on TSPLIB instances.

7.2.2 Experiment results

Table 2 shows the average best costs got by GLS and EB-GLS, in which the smaller cost values are in bold. The sign “+” indicates that EB-GLS significantly out-perform GLS using a Mann-Whitney U-test at the 0.05

Table 2 Comparison results on randomly generated instances, the better metric values are marked by bold texts

Instance	Average Best Cost		P-value
	GLS	EB-GLS	
randa10000	37928164	37849305 +	2.11e-20
randb10000	59934293	59808692 +	1.94e-21
randc10000	50040286	49922413 +	1.53e-27
randd10000	22909402	22857558 +	8.62e-25
rande10000	70175627	70019896 +	1.20e-23
randf10000	29017812	28955712 +	1.90e-26
randg10000	11929810	11900595 +	4.11e-29
randh10000	70408148	70248660 +	1.37e-25
randi10000	44957797	44848043 +	1.25e-29
randj10000	24271377	24207587 +	9.72e-30

significance level. From Table 2 we can see that the performance of EB-GLS is significantly better than that of GLS on all the 10 randomly generated instances.

7.3 Comparison with Ant Colony Optimization Algorithm

In this section, we compare the proposed EB-GLS with a TSP algorithm that employs completely different mechanism, the Ant Colony Optimization (ACO) algorithm [6]. ACO is widely used to solve the TSP since it is inspired by how ants find the shortest path to the food. Here we use the ACOTSP software package available at <http://www.aco-metaheuristic.org/aco-code/>. The comparison method is similar to the method we use in Section 7.1, but here we only use 10 test instances.

We set the parameters of ACO based on [24], which are shown in Table 3. The test instances we select are eil101, d198, kroA200, rd400, d657, u724, pcb1173, u1817, d2103 and u2319. The maximum runtime of each instance is same to the experiment setting in Section 7.1. The result data of EB-GLS also comes from the experiment in Section 7.1.

Table 4 show the comparison results between EB-GLS and ACOTSP where the bold font means that one algorithm gets a better metric value than the other one. We conduct Mann-Whitney U-test with a 0.05 significance level on the excess data and the runtime data respectively. Based on the metric values and the Mann-Whitney U-test, we conclude that EB-GLS out-performs

Table 3 Parameter settings of ACO

Parameters	Description	Values
m_{ACO}	Number of ants	25
α	Influence of pheromone trails	1
β	Influence of heuristic information	2
ρ	Pheromone trail evaporation	0.2
LS	Local search	3-Opt
MMAS	MAX-MIN ant system	Apply

Table 4 Comparison results between EB-GLS and ACOTSP on TSPLIB instances, the better metric values are marked by bold texts

Instance	Max Runtime (s)	Success of 100		Average Excess (%)		Excess P-value	Average Runtime (s)		Runtime P-value
		ACOTSP	EB-GLS	ACOTSP	EB-GLS		ACOTSP	EB-GLS	
eil101	11	100	100	0.0000	0.0000 \approx	-	0.05	0.02 +	1.73e-21
d198	20	76	96	0.0015	0.0004 +	1.12e-04	10.03	4.79 +	2.26e-08
kroA200	20	100	100	0.0000	0.0000 \approx	-	0.25	0.17 +	8.59e-15
rd400	40	90	93	0.0007	0.0005 \approx	3.51e-01	14.34	6.86 +	9.82e-11
d657	66	0	0	0.0557	0.0038 +	9.70e-21	66.00	66.00 \approx	-
u724	73	43	58	0.0261	0.0069 +	2.39e-05	56.85	50.43 +	2.76e-02
pcb1173	118	14	22	0.0252	0.0095 +	2.10e-04	111.64	103.85 +	2.56e-02
u1817	182	0	1	0.1563	0.1398 \approx	1.22e-01	182.00	181.93 +	2.38e-09
d2103	211	8	0	0.0402	0.1339 -	6.36e-12	203.81	211.00 -	7.67e-04
u2319	232	0	6	0.3068	0.0068 +	2.22e-38	232.01	227.16 +	5.06e-14

ACOTSP on nine instances, while ACOTSP out-performs EB-GLS on only one instances. Compared the results in Table 4 and the results in Table 1 (and Table 6 in the Appendix) we can see that, the original GLS performs worse than ACOTSP on several instances (e.g. rd400, u724 and pcb1173). Meanwhile the enhanced variant of GLS, EB-GLS, performs better than ACOTSP on those instances.

8 Conclusions

As an important part of memetic algorithm, LS usually finds locally optimal solutions. GLS is a simple yet powerful strategy to guide LS escape from locally optimal solutions in combinatorial optimization. Its success is due to its feature penalizing mechanism. It has been observed that many combinatorial optimization problems exhibit a big valley structure. This implies that solutions with higher quality have a better chance of being similar to other good solutions, even the global optima. To exploit this property, we have proposed a new variant of GLS, EB-GLS, with an improved feature penalizing mechanism. EB-GLS records and updates an elite solution, which is the best solution found so far during the search. Under the assumption that features present in the recorded elite solution are more likely to be part of a global optimum, EB-GLS reduces the probabilities of these features being penalized. In doing so, search efficiency can be significantly improved. We use symmetric TSP as the test problem to conduct experiments. Our objective is not to develop a new best algorithm for the TSP, but to show the effectiveness of our modification. We have conducted extensive experiments to study the behavior of EB-GLS on two TSP instance, att532 and u2319. The former instance has a big valley structure, while the latter instance does not. We also compare EB-GLS and GLS on a large number of test instances. Experimental results suggest that EB-GLS out-performs GLS on most instances, and EB-GLS's performance does not drastically deteriorate on the instance that does not have the big valley structure. Our work represents the first attempt of using big valley structure to improve GLS. In addition, we hope that the experimental methodology in this paper can inspire new methods to study penalization based algorithms.

Acknowledgements The work described in this paper was supported by a grant from ANR/RCC Joint Research Scheme sponsored by the Research Grants Council of the Hong Kong Special Administrative Region, China and France National Research Agency (Project No. A-CityU101/16).

References

1. Alhindi, A., Zhang, Q.: MOEA/D with guided local search: Some preliminary experimental results. In: Computer Science and Electronic Engineering Conference (CEECE), 2013 5th, pp. 109–114. IEEE (2013)
2. Alsheddy, A., Tsang, E.P.: Empowerment scheduling for a field workforce. *Journal of Scheduling* **14**(6), 639–654 (2011)
3. Basharu, M., Arana, I., Ahriz, H.: Distributed guided local search for solving binary discsp. In: FLAIRS Conference, pp. 660–665 (2005)
4. Bentley, J.J.: Fast algorithms for geometric traveling salesman problems. *ORSA Journal on Computing* **4**(4), 387–411 (1992)
5. Boese, K.D.: Cost versus distance in the traveling salesman problem. UCLA Computer Science Department (1995)
6. Dorigo, M., Birattari, M., Stützle, T.: Ant colony optimization. *IEEE Computational Intelligence Magazine* **1**(4), 28–39 (2006)
7. Eiben, Á.E., Van Der Hauw, J.K., van Hemert, J.I.: Graph coloring with adaptive evolutionary algorithms. *Journal of Heuristics* **4**(1), 25–46 (1998)
8. Hains, D.R., Whitley, L.D., Howe, A.E.: Revisiting the big valley search space structure in the TSP. *Journal of the Operational Research Society* **62**(2), 305–312 (2011)
9. Hasan, S.K., Sarker, R., Essam, D., Cornforth, D.: Memetic algorithms for solving job-shop scheduling problems. *Memetic Computing* **1**(1), 69–83 (2009)
10. Helsgaun, K.: An effective implementation of the lin–kernighan traveling salesman heuristic. *European Journal of Operational Research* **126**(1), 106–130 (2000)
11. Jadon, S.S., Bansal, J.C., Tiwari, R., Sharma, H.: Accelerating artificial bee colony algorithm with adaptive local search. *Memetic Computing* **7**(3), 215–230 (2015)
12. Jones, T.: Evolutionary algorithms, fitness landscapes and search. Ph.D. thesis, Citeseer (1995)
13. Jones, T., Forrest, S.: Fitness distance correlation as a measure of problem difficulty for genetic algorithms. In: Eshelman LJ (ed) Proceedings of the 6th international conference on genetic algorithms. Morgan Kaufmann, San Francisco, CA, pp. 184–192
14. Kauffman, S.A.: The origins of order: Self-organization and selection in evolution. Oxford University Press, USA (1993)
15. Lau, T., Tsang, E.P.K.: Guided genetic algorithm and its application to radio link frequency assignment problems. *Constraints* **6**(4), 373–398 (2001)
16. Lourenço, H.R., Martin, O.C., Stützle, T.: Iterated local search: Framework and applications. In: Handbook of Metaheuristics, pp. 363–397. Springer (2010)
17. Marinaki, M., Marinakis, Y.: A hybridization of clonal selection algorithm with iterated local search and variable neighborhood search for the feature selection problem. *Memetic Computing* **7**(3), 181–201 (2015)
18. Merz, P., Freisleben, B.: Fitness landscape analysis and memetic algorithms for the quadratic assignment problem. *IEEE Transactions on Evolutionary Computation* **4**(4), 337–352 (2000)
19. Merz, P., Freisleben, B.: Memetic algorithms for the traveling salesman problem. *Complex Systems* **13**(4), 297–346 (2001)
20. Merz, P., Katayama, K.: Memetic algorithms for the unconstrained binary quadratic programming problem. *BioSystems* **78**(1), 99–118 (2004)
21. Mester, D., Bräysy, O.: Active guided evolution strategies for large-scale vehicle routing problems with time windows. *Computers & Operations Research* **32**(6), 1593–1614 (2005)
22. Mills, P., Tsang, E., Ford, J.: Applying an extended guided local search to the quadratic assignment problem. *Annals of Operations Research* **118**(1), 121–135 (2003)

23. Ochoa, G., Veerapen, N.: Deconstructing the big valley search space hypothesis. In: *Evolutionary Computation in Combinatorial Optimization*, pp. 58–73. Springer (2016)
24. Oliveira, S.M., Hussin, M.S., Stützle, T., Roli, A., Dorigo, M.: A detailed analysis of the population-based ant colony optimization algorithm for the TSP and the QAP. In: *Proceedings of the 13th annual conference companion on Genetic and evolutionary computation*, pp. 13–14. ACM (2011)
25. Reeves, C.R.: Landscapes, operators and heuristic search. *Annals of Operations Research* **86**, 473–490 (1999)
26. Reinelt, G.: TspLib—a traveling salesman problem library. *ORSA Journal on Computing* **3**(4), 376–384 (1991)
27. Tao, X., Haubrich, H.J.: A hybrid metaheuristic method for the planning of medium-voltage power distribution systems (2005)
28. Tarantilis, C.D., Zachariadis, E.E., Kiranoudis, C.T.: A hybrid guided local search for the vehicle-routing problem with intermediate replenishment facilities. *INFORMS Journal on Computing* **20**(1), 154–168 (2008)
29. Vansteenwegen, P., Souffriau, W., Berghe, G.V., Van Oudheusden, D.: A guided local search metaheuristic for the team orienteering problem. *European Journal of Operational Research* **196**(1), 118–127 (2009)
30. Voudouris, C., Tsang, E.: Guided local search and its application to the traveling salesman problem. *European Journal of Operational Research* **113**(2), 469–499 (1999)
31. Voudouris, C., Tsang, E.P., Alsheddy, A.: Guided local search. In: *Handbook of Metaheuristics*, pp. 321–361. Springer (2010)
32. Zachariadis, E.E., Tarantilis, C.D., Kiranoudis, C.T.: A guided tabu search for the vehicle routing problem with two-dimensional loading constraints. *European Journal of Operational Research* **195**(3), 729–743 (2009)
33. Zhang, W.: Configuration landscape analysis and backbone guided local search.: Part i: Satisfiability and maximum satisfiability. *Artificial Intelligence* **158**(1), 1–26 (2004)
34. Zhong, Y., Cole, M.H.: A vehicle routing problem with backhauls and time windows: a guided local search solution. *Transportation Research Part E: Logistics and Transportation Review* **41**(2), 131–144 (2005)

Appendix

In Section 4, we state that att532 has the big valley structure, while u2319 does not have the big valley structure. Our statements are based on the landscape sampling experiment conducted on these two instances, in which 1,000 runs of GLS and 1,000 runs of EB-GLS are executed until finding the global optimum. During each run, the best solutions found so far are recorded and the final global optimum is also recorded. In fact, we conduct the same landscape sampling experiment on another eight instances. By analyzing the results, we conclude that all these eight instances satisfy the requirements of the big valley structure we defined in Section 4. Table 5 shows the landscape sampling results on these eight instances. Fig. 13 shows the scatter plots of the recorded best solutions found so far.

Table 5 The landscape sampling results on eight selected TSPLIB instances. N_{opt} is the number of the unique global optima found by these 2,000 runs. $D_{o,min}$ ($D_{o,avr}, D_{o,max}$) is the minimum (average, maximum) distance between the global optima. The last column is the FDC value of the recorded best solutions found so far during the 2,000 runs.

Instances	City Num	N_{opt}	$D_{o,min}$	$D_{o,avr}$	$D_{o,max}$	FDC
rd400	400	8	3	21	36	0.83
gr431	431	2	13	13	13	0.76
pcb442	442	2000	6	40	69	0.79
pa561	561	2000	6	44	82	0.83
u574	574	4	2	4	6	0.84
rat575	575	2	3	3	3	0.85
rat783	783	811	2	15	31	0.89
u1432	1432	2000	191	269	342	0.82

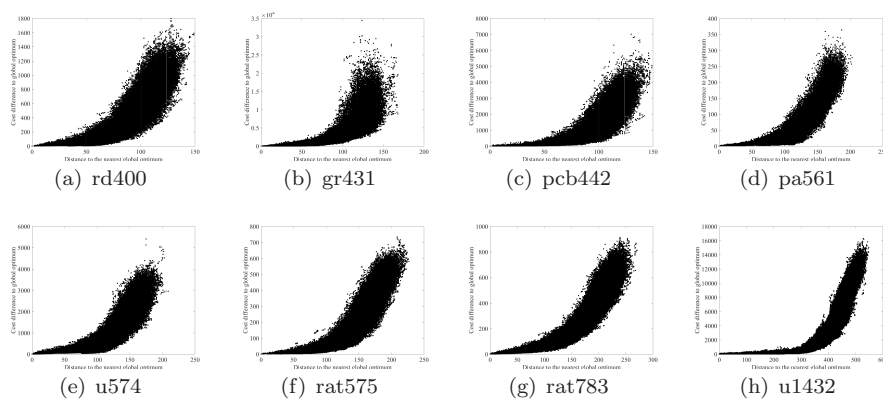


Fig. 13 The scatter plots of the recorded best solutions found so far during 1,000 runs of GLS and 1,000 runs of EB-GLS on eight selected instances. The cost difference to the globally optimal cost (vertical axis) is plotted against the distance to the nearest globally optimal solution (horizontal axis)

In Table 1 we present the comparison results between EB-GLS and GLS on the 33 TSPLIB instances with more than 1000 cities. Table 6 shows the comparison results on the other 76 TSPLIB instances with less than 1000 cities.

Table 6 Comparison results between EB-GLS and GLS on the TSPLIB instances with less than 1000 cities, the better metric values are marked by bold texts

Instance	Max Runtime (s)	Success of 100		Average Excess (%)		Excess P-value	Average Runtime (s)		Runtime P-value
		GLS	EB-GLS	GLS	EB-GLS		GLS	EB-GLS	
burma14	2	100	100	0.0000	0.0000 ≈	-	0.0000	0.0000 ≈	-
ulysses16	2	100	100	0.0000	0.0000 ≈	-	0.0000	0.0000 ≈	-
gr17	2	100	100	0.0000	0.0000 ≈	-	0.0000	0.0000 ≈	-
gr21	3	100	100	0.0000	0.0000 ≈	-	0.0000	0.0000 ≈	-
ulysses22	3	100	100	0.0000	0.0000 ≈	-	0.0000	0.0000 ≈	-
gr24	3	100	100	0.0000	0.0000 ≈	-	0.0000	0.0000 ≈	-
fri26	3	100	100	0.0000	0.0000 ≈	-	0.0002	0.0006 ≈	1.51e-01
bayg29	3	100	100	0.0000	0.0000 ≈	-	0.0006	0.0022 -	1.15e-03
bays29	3	100	100	0.0000	0.0000 ≈	-	0.0009	0.0007 ≈	6.05e-01
dantzig42	5	100	100	0.0000	0.0000 ≈	-	0.0006	0.0010 ≈	3.00e-01
swiss42	5	100	100	0.0000	0.0000 ≈	-	0.0016	0.0006 +	2.43e-02
att48	5	100	100	0.0000	0.0000 ≈	-	0.0048	0.0037 ≈	2.63e-01
gr48	5	100	100	0.0000	0.0000 ≈	-	0.0067	0.0042 ≈	1.86e-01
hk48	5	100	100	0.0000	0.0000 ≈	-	0.0017	0.0030 -	4.17e-02
eil51	6	100	100	0.0000	0.0000 ≈	-	0.0103	0.0106 ≈	9.98e-01
berlin52	6	100	100	0.0000	0.0000 ≈	-	0.0016	0.0010 ≈	2.09e-01
brazil58	6	100	100	0.0000	0.0000 ≈	-	0.0032	0.0031 ≈	7.99e-01
st70	7	100	100	0.0000	0.0000 ≈	-	0.0185	0.0119 +	5.81e-04
eil76	8	100	100	0.0000	0.0000 ≈	-	0.0099	0.0082 ≈	9.03e-02
pr76	8	100	100	0.0000	0.0000 ≈	-	0.0407	0.0148 +	8.73e-05
gr96	10	100	100	0.0000	0.0000 ≈	-	0.0262	0.0267 ≈	5.56e-01
rat99	10	100	100	0.0000	0.0000 ≈	-	0.0325	0.0191 +	9.54e-07
kroA100	10	100	100	0.0000	0.0000 ≈	-	0.0158	0.0103 +	4.46e-05
kroB100	10	100	100	0.0000	0.0000 ≈	-	0.0458	0.0280 +	7.80e-03
kroC100	10	100	100	0.0000	0.0000 ≈	-	0.0247	0.0069 +	2.55e-19
kroD100	10	100	100	0.0000	0.0000 ≈	-	0.0287	0.0133 +	4.78e-12
kroE100	10	100	100	0.0000	0.0000 ≈	-	0.0534	0.0314 +	2.02e-05
rd100	10	100	100	0.0000	0.0000 ≈	-	0.0354	0.0206 +	4.10e-07
eil101	11	100	100	0.0000	0.0000 ≈	-	0.0195	0.0204 ≈	9.70e-01
lin105	11	100	100	0.0000	0.0000 ≈	-	0.0202	0.0125 +	3.36e-06
pr107	11	100	100	0.0000	0.0000 ≈	-	0.7517	0.1438 +	2.35e-23
gr120	12	100	100	0.0000	0.0000 ≈	-	0.1438	0.0493 +	2.36e-15
pr124	13	100	100	0.0000	0.0000 ≈	-	0.0246	0.0337 -	3.15e-04
bier127	13	100	100	0.0000	0.0000 ≈	-	0.3955	0.1055 +	7.47e-21
ch130	13	100	100	0.0000	0.0000 ≈	-	0.0895	0.0642 +	1.67e-05
pr136	14	99	100	0.0001	0.0000 ≈	3.22e-01	1.7463	0.1631 +	3.44e-18
gr137	14	100	100	0.0000	0.0000 ≈	-	0.0907	0.0429 +	2.01e-17
pr144	15	100	100	0.0000	0.0000 ≈	-	0.0811	0.1134 -	3.58e-03
ch150	15	100	100	0.0000	0.0000 ≈	-	0.2003	0.1230 +	4.34e-07
kroA150	15	100	100	0.0000	0.0000 ≈	-	0.3707	0.0848 +	9.34e-14
kroB150	15	100	100	0.0000	0.0000 ≈	-	0.3672	0.2334 +	1.12e-06
pr152	16	100	100	0.0000	0.0000 ≈	-	1.8919	0.6639 +	1.68e-09
u159	16	100	100	0.0000	0.0000 ≈	-	0.0658	0.0628 ≈	9.21e-01
sil75	18	100	100	0.0000	0.0000 ≈	-	5.4633	1.8940 +	1.65e-20
brg180	18	100	100	0.0000	0.0000 ≈	-	0.0044	0.0049 ≈	8.02e-01
rat195	20	100	100	0.0000	0.0000 ≈	-	0.4984	0.2696 +	2.83e-05
d198	20	75	96	0.0016	0.0004 +	3.28e-05	14.7688	4.7853 +	2.51e-22
kroA200	20	100	100	0.0000	0.0000 ≈	-	1.7318	0.1695 +	1.26e-32
kroB200	20	100	100	0.0000	0.0000 ≈	-	1.2219	0.0886 +	5.37e-32
gr202	21	100	100	0.0000	0.0000 ≈	-	1.8843	0.6493 +	6.34e-19
ts225	23	100	100	0.0000	0.0000 ≈	-	0.7552	0.4194 +	4.46e-05
tsp225	23	99	100	0.0008	0.0000 ≈	3.22e-01	2.9281	0.6930 +	2.74e-15
pr226	23	93	98	0.0008	0.0006 ≈	9.29e-02	6.5625	3.0864 +	1.89e-08
gr229	23	89	100	0.0010	0.0000 +	6.76e-04	8.0847	1.2958 +	1.25e-22
gil262	27	100	100	0.0000	0.0000 ≈	-	2.3682	1.0298 +	3.09e-10
pr264	27	100	100	0.0000	0.0000 ≈	-	0.9685	0.4527 +	1.68e-15
a280	28	100	100	0.0000	0.0000 ≈	-	0.1767	0.1731 ≈	3.19e-01
pr299	30	94	100	0.0001	0.0000 +	1.33e-02	9.7268	0.4571 +	1.12e-31
lin318	32	100	100	0.0000	0.0000 ≈	-	2.3201	1.2127 +	8.33e-09
rd400	40	87	93	0.0009	0.0005 ≈	1.59e-01	20.4316	6.8556 +	2.67e-19
fl417	42	1	83	0.0333	0.0123 +	1.05e-18	41.7864	18.7175 +	2.85e-29
gr431	44	4	71	0.0072	0.0005 +	3.25e-28	43.1186	22.0183 +	9.38e-22
pr439	44	1	58	0.0598	0.0140 +	3.97e-26	43.8654	26.0844 +	3.09e-18
pcb442	45	28	94	0.0087	0.0014 +	1.22e-18	37.2381	8.9825 +	2.66e-24
d493	50	1	15	0.0135	0.0065 +	2.10e-20	49.9264	47.3198 +	2.66e-04
att532	54	6	98	0.0229	0.0012 +	1.33e-32	52.0478	10.4495 +	1.17e-35
ali535	54	0	96	0.0337	0.0010 +	2.81e-36	54.0000	16.4560 +	1.12e-36
si535	54	0	2	0.2140	0.0387 +	1.77e-33	54.0000	53.4750 ≈	1.58e-01
pa561	57	69	99	0.0119	0.0004 +	7.99e-09	33.7124	10.0504 +	7.84e-20
u574	58	31	100	0.0076	0.0000 +	2.44e-23	50.9637	7.4151 +	3.01e-34
rat575	58	6	53	0.0337	0.0080 +	4.89e-24	57.1423	38.1065 +	8.13e-14
p654	66	0	5	0.1657	0.0461 +	1.30e-31	66.0000	65.1685 +	2.42e-02
d657	66	0	0	0.0258	0.0038 +	1.68e-31	66.0000	66.0000 ≈	-
gr666	67	0	25	0.0417	0.0158 +	1.81e-16	67.0000	59.0446 +	1.07e-07
u724	73	2	58	0.0428	0.0069 +	3.68e-26	72.5028	50.4334 +	1.59e-17
rat783	79	24	100	0.0151	0.0000 +	1.07e-26	70.4217	11.3429 +	6.42e-35